On instabilities of growing bi-material interfaces

Reheman, Wureguli; Ståhle, Per; Kao-Walter, Sharon

ICSI 2019 The 3rd International Conference on Structural Integrity

On instabilities of growing bi-material interfaces

W. Reheman[1] & P. Ståhle[2] & S. Kao-Walter[1]

[1] *Dept. Mechanical Engineering, Blekinge Institute of Technology, SE-371 79 Karlskrona, Sweden*
[2] *Division of Solid Mechanics, LTH, Lund University, Box 118, SE-221 00 Lund, Sweden*

Abstract

This study concerns with the evolution of morphological patterns that often arise on the interface of bi-material, so called metal-precipitate phase, due to the instability of the interfaces. The instability leads to growth or retraction of small perturbation, which may determine the formation of a variety of morphological patterns initially arising on surfaces of growing precipitates at small length scales. To better understand the cause of different patterns on the bi-material interfaces, an analytical study of the stability of the precipitate-matrix interface is performed. First, a wavy interface perturbation is used to examine the spontaneous variations that occur at the precipitate-matrix interface. Then, the analysis utilises Cerruti?s solution to compute the perturbed stress field surrounding the interface. It is shown that a virtually flat interface subjected to tension is in general unstable. The amplitude of sinusoidal perturbations decays for short wave lengths and grow for longer wave lengths. Both a critical wave length for which the perturbation amplitude is unaffected and a specific ditto which obtain maximum perturbation growth rate are derived

Keywords: Bi-material, Instability, Waviness; Growth rate;

1. Introduction

A variety of morphological patterns initially arise on the surfaces of growing precipitates at small length scales if the nuclei overcome certain energy barrier. The patterns could be ridges, wrinkles or fringes, etc. Fig. 1 show platelets forming at the interface of a zirconium hydride precipitate formed in zirconium metal containing high concentration of hydrogen, cf. Singh et al. (2006). Formation of these patterns directly influence the final shape of precipitates and the morphological and micro-structural differences of precipitates affect the fracture process and has consequences for the strength of the material. The initial cause of these morphological pattern is assumed to be due to the instability of the interface between precipitates and the original matrix.

There have been several approaches to study the interface instability in the past by Grinfeld (1993); Asaro and Tiller (1972). These studies are rather general approaches related with the instability of bi-materials, and less related

---

* Wureguli Reheman. Tel.: +46-707668603
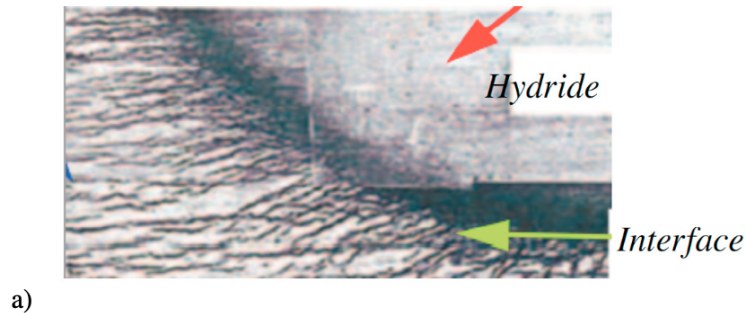 *E-mail address:* wureguli.reheman@bth.se

a)

Fig. 1. Zirconium hydride precipitate situated at the surface of a zirconium alloy tube. The tube was exposed to a hydrogen rich environment. cf. Singh et al. (2006).

to the case that one material expands while the both materials are exposed to remote stress field. The expansion of the material may alter a lot the situation at the interface as compared because of large local variation of the stress field. In the studies of Reheman (2017); Ståhle and Reheman (2016), this situation is taken into consideration and implemented numerically by using a phase field method.

In the present study, an analytical study of the interface instability which leads to the growth and retraction of waviness between metal and precipitate interface is performed. The effect of expansion of precipitates is included in the derivation of stress distribution of a perturbed plane bi-material interface. It is implemented when utilising a classic formulation of the Cerruti's solution for half space subjected to a tangential surface line-load, cf. Fung (1965). The body under consideration is subjected to uniaxial stretching. The solution cover both plane stress and plane strain.

2. Analytical model for wavy interface and results

Consider a body with a virtually flat bi-material interface, the materials A and B on each side of the interface have identical elastic material properties with the elastic modulus E' and Poisson's ratio ν'. A Cartesian coordinate system is attached to the bi-material interface with the x_2-direction along the normal of the interface. Without loss of generality a plane stress case is studied. The solution of the corresponding plane strain case is obtained simply by replacing E', ν' and the expansion strain ϵ'_s with the following

$$E' = \begin{cases} E & \text{plane stress} \\ E/(1-\nu^2) & \text{pl. strain} \end{cases}, \quad \nu' = \begin{cases} \nu & \text{pl. stress} \\ \nu/(1-\nu) & \text{pl. strain} \end{cases} \quad \text{and} \quad \epsilon'_s = \begin{cases} \epsilon_s & \text{pl. stress} \\ \epsilon_s/(1+\nu) & \text{pl. strain} \end{cases}. \quad (1)$$

Prior to the phase transformation, the entire body is stretched ϵ_∞ in the x_1-direction by a uniaxial stress $\sigma_{11} = \sigma_\infty/E'$. The only difference between the upper and lower half-spaces is that the one occupying the lower half-space, $x_2 < 0$, after a phase transformation in the absence of tractions, obtains a uniform expansion of ϵ'_s. Thus, the phase transformation decreases the stress in the lower half space with $-(\epsilon'_s/2)E'$, and increases it in the upper half-space with $(\epsilon'_s/2)E'$. All other stresses vanish as long as the interface is perfectly flat.

Spontaneous variations at the interface will perturb the interface in between the two materials. Therefore, we introduce a sinusoidally wavy interface (cf. Fig. 2a). The wave amplitude is considered to be infinitesimal.

The analyses are based on a series of fictitious events that will simplify the mathematical treatment. The starting point is a perfectly bonded bi-material body (see Fig. 2a), where the matrix occupies the upper part (A) of the body and the precipitate occupies the lower part (B). At the first step, the body is cut and separated along the perturbed interface, Fig. 2b. To maintain the homogeneous mechanical state of the separated parts, tractions have to be applied on the upper and lower parts of the interface respectively. If the upper and lower wavy surfaces are approached from each side the stresses are,

$$\sigma_{11}^A = \sigma_{11}^B = \sigma_\infty, \text{ and } \sigma_{22}^B = \sigma_{22}^A = \sigma_{12}^B = \sigma_{12}^A = 0. \quad (2)$$
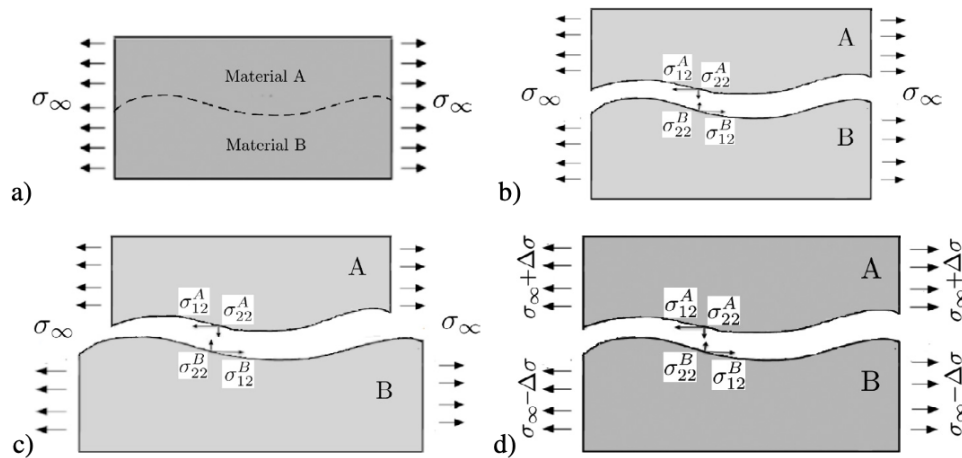
Fig. 2. a) Perfectly bonded with wavy interface, b) first step, separation along the interface, c) second step, expanded lower half-space B, d) adjusted remote stresses $\Delta\sigma = \epsilon_\infty E/2$ to make parts A and B compatible.
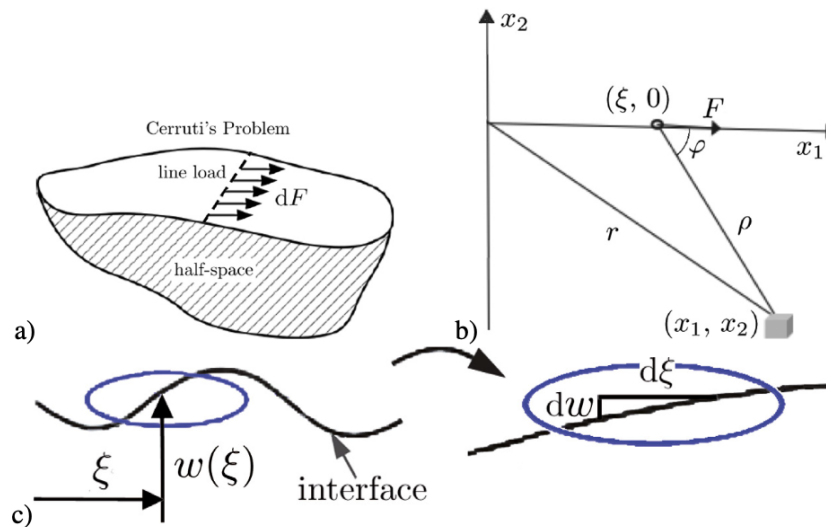

Fig. 3. a) a point force tangential to the boundary over an area S, b) on coordinates, a) ??? $a(\xi)$ should be $w(\xi)$ close up on wavy surface

In the second step, the lower part B receives additional strain ϵ_s'. Stress is not affected, but the material fragments A and B does not fit together. Finally the remote stress σ_{11} is adjusted to make parts A and B compatible. To maintain equal normal stress σ_∞, the stress adjustment in part A and B is the same amount but with an opposite sign,

$$\sigma_{11}^A = \sigma_\infty + E'\epsilon_s'/2, \quad \sigma_{11}^B = \sigma_\infty - E'\epsilon_s'/2, \quad \sigma_{22}^B = \sigma_{22}^A = \sigma_{12}^B = \sigma_{12}^A = 0. \tag{3}$$

Because of the symmetries across $x_2 = 0$, the analysis is reduced to a study of the half-plane B only. The position of the perturbed interface is given by the function $w(\xi)$ as indicated in Fig. 3c. From Eq. (3) above the force dF, force per unit of length that act on the upper surface of B at $x_1 = \xi$ is $dF = \sigma_{11}^B dw$, cf. Fig. 3a to c. The resulting stress distribution due to dF as in Fig. 3a, is given by Cerruti, cf. Fung (1965), as the following

$$d\sigma_{\rho\rho} = -\frac{\pi}{2}\frac{dF\cos\varphi}{\rho} = -\frac{\pi}{2}\frac{dF(x_1 - \xi)}{\rho^2}, \tag{4}$$

and all other stress contributions vanish. The polar coordinates are defined in Fig. 3a.

The polar coordinate system is attached to the origin of the Cartesian coordinate system, $x_1 = x_2 = 0$, and $\rho = \sqrt{(x_1 - \xi)^2 + x_2^2}$ and $\varphi = \arctan[x_2/(x_1 - \xi)]$, according to Fig. 3b. The force is defined as the tangential traction

required to maintain a homogeneous stress state in the respective half-space. The attempt is to calculate the growth rate of sinusoidal perturbations given by

$$w(\xi) = a \sin k\xi \quad \text{and} \quad \frac{\mathrm{d}w}{\mathrm{d}\xi} = ak \cos k\xi, \tag{5}$$

where k is the wave number. Thus, the force contribution from the traction $\mathrm{d}F$ applied on the lower part B, at $x_1 = \xi$ becomes

$$\mathrm{d}F = (\sigma_\infty - \frac{1}{2}E'\epsilon_s')\mathrm{d}w = (\sigma_\infty - \frac{1}{2}E'\epsilon_s')\frac{\mathrm{d}w}{\mathrm{d}\xi}\mathrm{d}\xi = (\sigma_\infty - \frac{1}{2}E'\epsilon_s')ak \cos x_1 k\mathrm{d}\xi, \tag{6}$$

cf. Fig. (3c).

Transformation from polar to Cartesian coordinates the following gives

$$\sigma_{11} = \sigma_{\rho\rho} \cos^2 \varphi, \quad \sigma_{22} = \sigma_{\rho\rho} \sin^2 \varphi, \quad \text{and} \quad \sigma_{12} = -\sigma_{\rho\rho} \sin 2\varphi. \tag{7}$$

By using Eqs. (4), (6), (7) and that $\cos \varphi = (x_1 - \xi)/\rho$, $\sin \varphi = -x_2/\rho$ and $\rho = \sqrt{(x_1 - \xi)^2 + x_2^2}$, the following total stresses are obtained after integration along the entire interface,

$$\sigma_{11} = (\sigma_\infty - \frac{1}{2}E'\epsilon_s')\left(1 - \frac{\pi}{2}akI_{11}\right), \sigma_{22} = -(\sigma_\infty - \frac{1}{2}E'\epsilon_s')\frac{\pi}{2}akI_{22}, \text{ and } \sigma_{12} = -(\sigma_\infty - \frac{1}{2}E'\epsilon_s')\frac{\pi}{2}akI_{12}, \tag{8}$$

where

$$\begin{aligned}
I_{11} &= \int_{-\infty}^{+\infty} \cos(k\xi)\frac{(x_1-\xi)^3}{\rho^4}\mathrm{d}\xi = \frac{\pi}{2}(2 + x_2k)e^{x_2k} \sin x_1k, \\
I_{22} &= \int_{-\infty}^{+\infty} \cos(k\xi)\frac{(x_1-\xi)x_2^2}{\rho^4}\mathrm{d}\xi = -\frac{\pi}{2}x_2ke^{x_2k} \sin x_1k, \\
I_{12} &= -\int_{-\infty}^{+\infty} \cos(k\xi)\frac{(x_1-\xi)^2x_2}{\rho^4}\mathrm{d}\xi = -\frac{\pi}{2}(1 + x_2k)e^{x_2k} \cos x_1k.
\end{aligned} \tag{9}$$

The calculations requires integration by parts. The relations $\int_{-\infty}^{\infty} \frac{t\cos t}{t^2+q^2}\mathrm{d}t = 0$ and $\int_{-\infty}^{\infty} \frac{t\sin t}{t^2+q^2}\mathrm{d}t = \pi e^{-|q|}$ become useful.

3. Gibbs' Free Energy Density

Both the elastic energy density, W, and the required interfacial energy, γ, increase with the wave number, k. The growth rate of the waviness of an interface that is sinusoidal positioned at $x_2 = a\sin(kx_1)$ is controlled by the availability of free energy. In the absence of no other energy resources than U and γ that seems reasonable to consider, the rate of growth of the waviness is assumed to be proportional to the excess of free energy due to a change of the wave amplitude. With the proportionality factor, L, being a non-negative constant the following is obtained,

$$\frac{\partial a}{\partial t} = L\frac{\partial}{\partial a}(W - \gamma), \tag{10}$$

in accordance with Landau and Lifshitz (1935).

3.1. Free elastic energy

The remote normal stress, $\sigma_\infty \pm E\epsilon_s/(1 - \nu^2)$, plus or minus depending in the specific half-plane, is assumed to dominate everywhere. Due to the wavy interface with a small amplitude $a \ll 1/k$, there will be a small perturbation of the stresses and strains of the order of ka. These stresses are significant only in the vicinity of the interface. The assumed plane stress, i.e., $\sigma_{13}=\sigma_{23}=\sigma_{33}=0$, reduces the involved stress components to those only in the x_1-x_2 plane.

The elastic energy density per unit volume for plane stress is defined by

$$W = \frac{\sigma_{ij}\epsilon_{ij}}{2} = \frac{1}{2E'}\left(\sigma_{11}^2 + \sigma_{22}^2 - 2\nu'\sigma_{11}\sigma_{22} + (1 + \nu')\sigma_{12}^2\right), \tag{11}$$

where the tensor notation for summation over equal indices is used.

The average elastic energy density, W_o, for a flat interface is

$$W_o = \frac{1}{2E'}\left(\sigma_\infty^2 - \frac{1}{2}E'\epsilon_s'\right)^2. \tag{12}$$

Insertion of Eqs. (8), (9) gives

$$W = \frac{1}{2E'}(\sigma_\infty - \frac{1}{2}E'\epsilon_s')^2\left((1 - \frac{\pi}{2}akI_{11})^2 + (\frac{\pi}{2}akI_{22})^2 - 2\nu'(1 - \frac{\pi}{2}akI_{11})\frac{\pi}{2}akI_{22} + (1 + \nu')(\frac{\pi}{2}akI_{12})^2\right). \tag{13}$$

Terms independent of the perturbation amplitude a does not contribute to the growth rate as it is readily seen in Eq. (10). Other terms only containing a single integral I_{11}, I_{22} or I_{12} become proportional to either $\cos x_1 k$ or $\sin x_1 k$ and vanish therefore, as an average over each period length $2\pi/k$, which leave us with

$$W' = \frac{1}{2E'}(\sigma_\infty - \frac{1}{2}E'\epsilon_s')^2(\frac{\pi}{2}ak)^2\left(I_{11}^2 + I_{22}^2 - 2\nu'I_{11}I_{22} + (1 + \nu')I_{12}^2\right). \tag{14}$$

Integration over the period $0 \le x_1 \le 2\pi/k$ and the entire lower half-plane gives an average per period

$$\frac{k}{2\pi}\int_0^{2\pi/k} I_{11}^2 dx_1 = \frac{\pi^2}{8}(2 + x_2 k)^2 e^{2x_2 k}, \quad \frac{k}{2\pi}\int_0^{2\pi/k} I_{22}^2 dx_1 = \frac{\pi^2}{8}x_2^2 k^2 e^{2x_2 k},$$
$$\frac{k}{2\pi}\int_0^{2\pi/k} I_{11}I_{22} dx_1 = 0 \text{ and } \frac{k}{2\pi}\int_0^{2\pi/k} I_{12}^2 dx_1 = \frac{\pi^2}{8}(1 + x_2 k)^2 e^{2x_2 k}. \tag{15}$$

Integration over the entire lower half-plane finally gives

$$\frac{k}{2\pi}\int_{-\infty}^{+\infty}\int_0^{2\pi/k} I_{11}^2 dx_1 dx_2 = \frac{5\pi^2}{32}, \quad \frac{k}{2\pi}\int_{-\infty}^{+\infty}\int_0^{2\pi/k} I_{22}^2 dx_1 dx_2 = \frac{\pi^2}{32k}, \text{ and } \frac{k}{2\pi}\int_{-\infty}^{+\infty}\int_0^{2\pi/k} I_{12}^2 dx_1 dx_2 = \frac{\pi^2}{32k}. \tag{16}$$

Thus, the elastic strain energy area density is summarised to

$$W' = \left(\frac{\pi}{4}\right)^4 \frac{7 + \nu'}{E'}(\sigma_\infty - \frac{1}{2}E'\epsilon_s')^2 a^2 k. \tag{17}$$

3.2. Interfacial energy density

A wavy interface that is sinusoidally positioned at $w = a\sin(x_1 k)$ have an area average calculated for a period length $2\pi/k$,

$$A = A_o \frac{k}{2\pi}\int_0^{2\pi/k} \sqrt{(dx_1)^2 + (dw)^2} = A_o\sqrt{1 + (dw/dx_1)^2} = A_o(1 + \frac{a^2 k^2}{2}\cos^2 x_1 k) + O(ak)^3, \tag{18}$$

where A_o is the area of the original flat interface. For small values of $dw/dx_1 \ll 1$ the following change of interfacial energy is obtained

$$\gamma = \gamma_o A/A_o = \gamma_o + \gamma_o \frac{a^2 k^2}{2}\int_0^{2\pi/k}\cos^2(kx_1)dx_1 = \gamma_o(1 + \frac{1}{4}\gamma_o a^2 k^2), \tag{19}$$

where γ_o is the flat interface energy which is assumed to be constant per unit of true area. The waviness causes an increase of the interface energy γ as it appears on a structural length scale.

4. Discussion and Conclusions

The growth rate according to Eq.(10) with the insertion of Eqs. (17) and (19) gives

$$\frac{\partial a}{\partial t} = L\frac{\partial}{\partial a}(W - \gamma) = L a k\left\{\frac{\pi^4}{64}\frac{7 + \nu'}{E'}\left(\sigma_\infty^2 + (\frac{1}{2}E'\epsilon_s')^2\right) - \frac{1}{2}\gamma_o k\right\}. \tag{20}$$
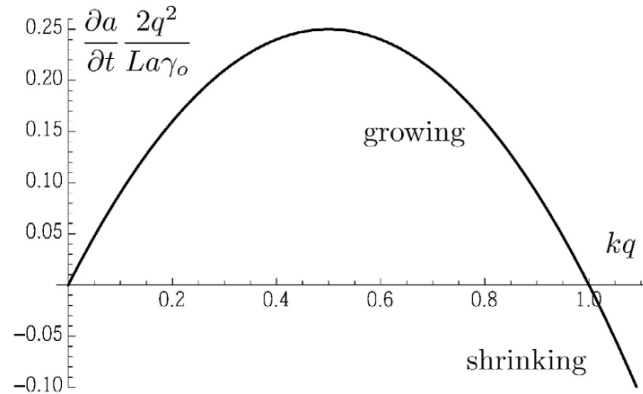
Fig. 4. Growth rate versus wave number. The scaling $q = (\frac{32}{\pi^4}\frac{\gamma_o E'}{7+\nu'})/\left(\sigma_\infty^2 + (\frac{1}{2}E'\epsilon_s')^2\right)$.
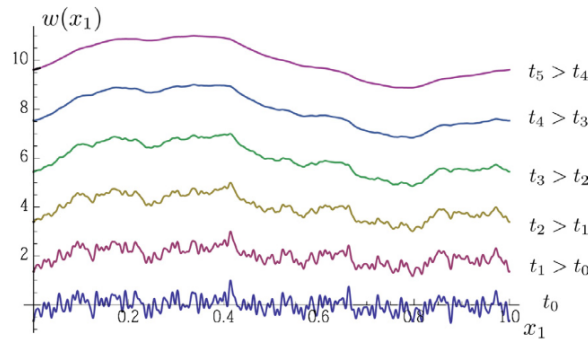

Fig. 5. Fictive perturbed surface where the higher wave numbers are getting filtered according to Eq. (21).

With a convenient scaling, the growth rate is written

$$\frac{\partial a}{\partial t}\frac{2q^2}{La\gamma_o} = kq(1 - kq), \quad \text{where} \quad q = (\frac{32}{\pi^4}\frac{\gamma_o E'}{7 + \nu'})/\left(\sigma_\infty^2 + (\frac{1}{2}E'\epsilon_s')^2\right). \tag{21}$$

The result is plotted in Fig. 4 shows that growth only occurs for interface waves with wave numbers below a critical value, i.e., sufficiently large wave lengths. It is readily observed in Eq. (20) that growth of perturbations occur a range of wave number range $0 < k < \frac{\pi^4}{32}\frac{7+\nu'}{\gamma_o E'}\left(\sigma_\infty^2 + (\frac{1}{2}E'\epsilon_s')^2\right)$. Maximum growth rate is at $k = \frac{\pi^4}{64}\frac{7+\nu'}{E'\gamma_o}\left(\sigma_\infty^2 + (\frac{1}{2}E'\epsilon_s')^2\right)$.

Above the critical value $k = \frac{\pi^4}{32}\frac{7+\nu'}{E'\gamma_o}\left(\sigma_\infty^2 + (\frac{1}{2}E'\epsilon_s')^2\right)$ perturbations do not grow, but instead decay with time and eventually become insignificant. It is also interesting to observe that the growth rate vanishes for vanishing wave numbers, meaning that a precipitate with a fluctuating but almost flat interface does not grow a waviness when only subjected to elastic and interfacial energy. These results are summarised in Fig. 4. Other energy sources such as those connected to chemical reactions or crystallographic alterations are believed not to contribute to the development of the surface waviness.

Figure 5 shows an example of growing perturbations of an interface. The initial generate interface is equipped with waves with wave number up to 10 times the critical wave number. At consecutive times the curve is shown to become smoother as the waves outside the range of permissible wave numbers are diluted. The growth of the remaining waves is conserving the profile as the amplitude increases. The appearance is expected as the distribution of wave numbers assumes a profile such as in Fig. 4.

Acknowledgement

References

Asaro, R., Tiller, W., 1972. Interface morphology development during stress corrosion cracking: Part i. via surface diffusion. Metallurgical and Materials Transactions B 3, 1789–1796.

Fung, Y., 1965. Foundations of Solid Mechanics. Prentice-Hall, Inc., New Jersey.

Grinfeld, M., 1993. The stress driven instability in elastic crystals: Mathematical models and physical manifestations. Journal of Nonlinear Science 3, 35–83.

Landau, L., Lifshitz, E., 1935. On the theory of the dispersion of magnetic permeability in ferromagnetic bodies. Phys Zeit Sowjetunion 8, 153.

Reheman, W., 2017. Mechanical Behaviour of Growing Precipitates. Division of Solid Mechanics, Lund University.

Singh, R.N., Ståhle, P., Banks-Sills, L., 2006. Fracture of zr-alloy pressure tubes due to hydride blister formation, Nordic Seminar on Computational Mechanics, Lund Institute of Technology. pp. 99–103.

Ståhle, P., Reheman, W., 2016. Interface instabilities of growing hydrides. Procedia Structural Integrity 2, 589–596.